Design of Line Source Antennas for Difference Patterns with Sidelobes of Individually Arbitrary Heights

ROBERT S. ELLIOTT, FELLOW, IEEE

Abstract—**A design method previously developed to give a sum pattern with arbitrary sidelobe topography is shown to be applicable to difference patterns as well. The basis is Bayliss patterns (Taylor-type patterns for the difference mode) which are transformed through an iterative procedure to the desired result. For practical cases the convergence is rapid and a previously developed do-loop computer program has been modified to facilitate the computations and provide final patterns and aperture distributions.**

Introduction

A CLASSIC procedure for the design of continuous line sources which yield a sum pattern consisting of a narrow main beam and symmetric low sidelobes has been formulated by Taylor [1]. The typical Taylor pattern has, in addition to the central main beam, a specified number of near-in sidelobes on each side which are essentially at a common, controlled height, with far-out sidelobes which decay in height as a function of angular distance from the main beam. The corresponding aperture distribution is symmetric in amplitude (nonzero everywhere, including endpoints) and uniform in phase when the main beam is broadside. A Taylor pattern is representable as a canonical product of factors whose roots are the zeros of the pattern.

Bayliss [2] has extended Taylor's technique to the case of the difference pattern. A typical Bayliss pattern consists of a pair of central main lobes plus a specified number of near-in sidelobes which are essentially at a common, controlled height, with far-out side lobes which decay in height as a function of angular distance from the main beam. The corresponding aperture distribution is symmetric in amplitude (nonzero everywhere except the midpoint) and uniform in phase over each half of the aperture, there being a 180° phase reversal between halves.

Previous papers [3], [4] have dealt with extensions of Taylor's method to the cases of 1) sum patterns with asymmetric sidelobes and 2) sum patterns with arbitrary sidelobe topography. The asymmetric sidelobe case was handled by modifying the Taylor canonical product so that its negative-root factors corresponded to a different sidelobe level than did its positive-root factors. Arbitrary sidelobe topography was accomplished by a perturbation technique which transforms a starting pattern through a series of iterations in which a do-loop computer program plays a major role.

Manuscript received July 15, 1975; revised November 23, 1975. This work was supported by the Hughes Aircraft Company.

The author is with the Department of Electrical Sciences, University of California, Los Angeles, CA and is also a consultant to the Hughes Aircraft Company, Canoga Park, CA 91304.

Since the Bayliss pattern is also representable as a canonical product of factors whose roots are the zeros of the pattern, it seemed clear that a simple modification should yield difference patterns with asymmetric sidelobes. More generally, it was also anticipated that Bayliss patterns could be perturbed to give arbitrary sidelobe topography, using the same iterative procedure which had proved successful in the case of sum patterns. This was found to be the case and the sections which follow detail the extension of the perturbation procedure to the general problem of modifying a Bayliss difference pattern in order to produce sidelobes of individually arbitrary heights.

Bayliss Patterns

A conventional Bayliss difference pattern [2, p. 649] is expressible in the form

$$F_0(z) = \pi z \cos \pi z \frac{\prod_{n=1}^{\bar{n}-1} \left[1 - \left(\frac{z}{\sigma Z_n}\right)^2\right]}{\prod_{n=0}^{\bar{n}-1} \left[1 - \left(\frac{z}{n+\frac{1}{2}}\right)^2\right]} \tag{1}$$

in which $z = (2a/\lambda) \cos \theta$, with $2a/\lambda$ the aperture extent in wavelengths, and with θ the angle measured from endfire. The parameters Z_n are given by

$$Z_n = \begin{cases} 0, & n = 0 \\ \xi_n, & n = 1,2,3,4 \\ \sqrt{A^2 + n^2}, & n = 5,6,\cdots \end{cases} \tag{2}$$

wherein A is a constant related to the sidelobe level, as will be elaborated shortly. $\bar{n}$ is a transition integer such that the innermost $\bar{n} - 1$ sidelobes on each side of the twin main lobes in the difference pattern are essentially at a common height, whereas the $\bar{n}$th sidelobe and all others further out decay as z^{-1}. The parameter σ is defined by

$$\sigma = \frac{\bar{n} + \frac{1}{2}}{Z_{\bar{n}}} \tag{3}$$

and serves to space the close-in nulls so that they blend smoothly with the sequence of far-out nulls.

Bayliss has shown that the parameters A and ξ_n can be related to the desired sidelobe level quite accurately by fourth-degree polynomials [2, p. 632]. When one uses his polynomial coefficients, computed values of A and ξ_n can be constructed, as shown in Table I.

After $\bar{n}$ and the sidelobe level are selected, Table I and (2) and (3) can be used to determine all the parameter values

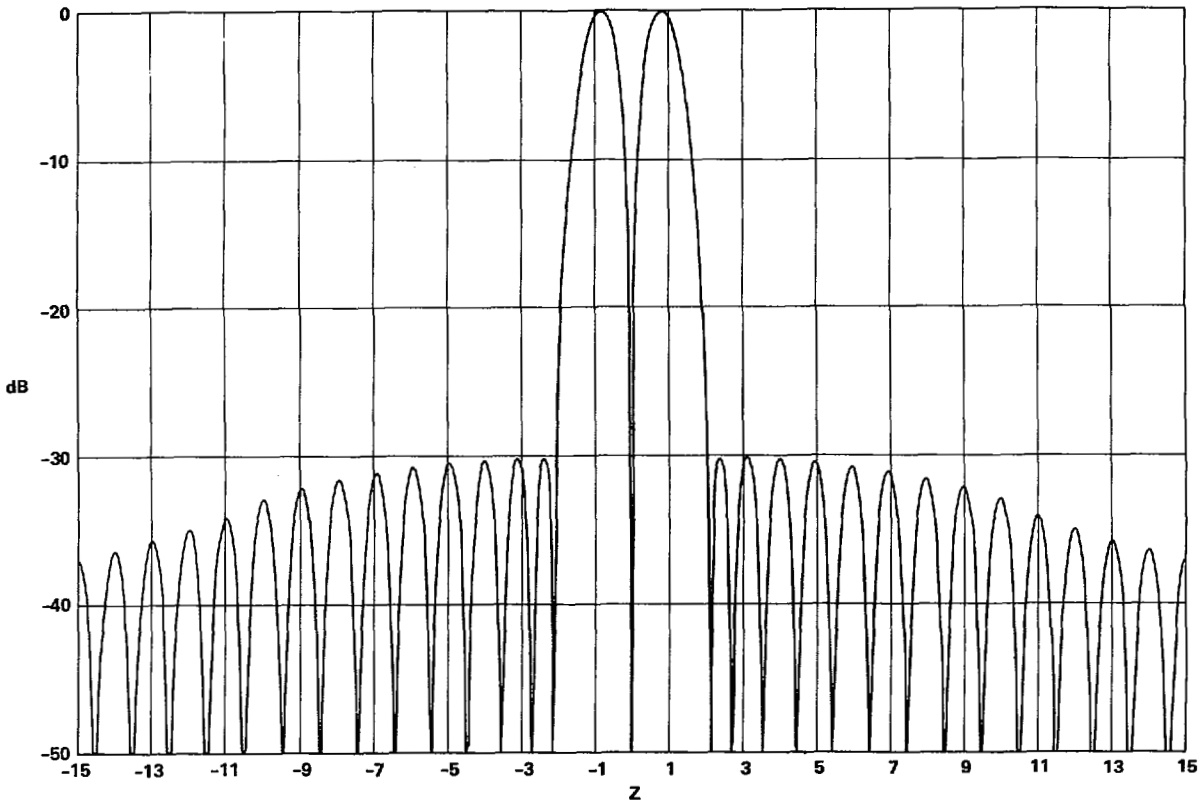

Fig. 1. Conventional Bayliss pattern with 30 dB sidelobes.

TABLE I
PARAMETER VALUE VERSUS SIDELOBE LEVEL FOR BAYLISS DIFFERENCE PATTERN

	Sidelobe Level in dB					
	15	20	25	30	35	40
A	1.0079	1.2247	1.4355	1.6413	1.8431	2.0415
ξ_1	1.5124	1.6962	1.8826	2.0708	2.2602	2.4504
ξ_2	2.2561	2.3698	2.4943	2.6275	2.7675	2.9123
ξ_3	3.1693	3.2473	3.3351	3.4314	3.5352	3.6452
ξ_4	4.1264	4.1854	4.2527	4.3276	4.4093	4.4973

needed in (1), so that a pattern can be computed. As an example, if $\bar{n} = 10$ and a sidelobe level of 30 dB is desired, then $A = 1.6413$ and $Z_{10} = \sqrt{A^2 + 100} = 10.1338$. Thus $\sigma = 10.5/Z_{10} = 1.0361$, and the roots needed in (1) are as given in Table II. When $F_0(z)$ is computed from (1) using these entries, the result is as shown in Fig. 1. One can observe the features that are generally present in a Bayliss pattern—two symmetrical center lobes, surrounded by symmetrical sidelobes. The near-in sidelobes tail-off only slightly from the design level, and the far-out sidelobes diminish in height as z^{-1}. It is this prototype pattern that we wish to modify.

DIFFERENCE PATTERNS WITH ARBITRARY SIDE LOBE TOPOGRAPHY

The perturbation procedure developed in [4], and which served to convert a starting sum pattern to a desired sum pattern, can be used (with some modifications) to accomplish the same objective when dealing with difference patterns.

Equation (1) can be generalized and written in the form

$$F_0(z) = C_0 \cos \pi z \frac{\prod_{n=-(\bar{n}_L-1)}^{\bar{n}_R-1} (z_n^0 - z)}{\prod_{n=0}^{\bar{n}_R-1} \left(1 - \frac{z}{n+\frac{1}{2}}\right) \prod_{n=0}^{\bar{n}_L-1} \left(1 + \frac{z}{n+\frac{1}{2}}\right)} \tag{4}$$

in which C_0 is a constant, and in which

$$\begin{aligned} z_n^0 &= \sigma_R Z_{n,R}, \qquad n = 1, 2, \cdots, \bar{n}_R - 1 \\ z_n^0 &= -\sigma_L Z_{n,L}, \qquad n = -1, -2, \cdots, -(\bar{n}_L - 1) \\ z_0^0 &= 0. \end{aligned} \tag{5}$$

The parameters $Z_{n,R}$ and $Z_{n,L}$ are given by (2), but with different values of A (call them A_R and A_L) corresponding

TABLE II
ROOTS OF THE BAYLISS 30/30 PATTERN

n	1	2	3	4	5	6	7	8	9
σZ_n	2.1456	2.7224	3.5553	4.4838	5.4525	6.4450	7.4494	8.4614	9.4787

TABLE III
AMPLITUDES AND POSITIONS OF LOBE PEAKS IN BAYLISS 30/30 PATTERN

$\|m\|$	1	2	3	4	5	6	7	8	9	10
$\|y_m\|$	0.8216	2.3846	3.1205	4.0104	4.9620	5.9432	6.9413	7.9488	8.9620	9.9785
$\|\eta_m{}^0\|$	1.0	0.0308	0.0309	0.0305	0.0297	0.0288	0.0276	0.0262	0.0244	0.0224

to the desired right-hand and left-hand sidelobe levels. (The requisite values of A_R and A_L can be read from Table I along with the companion values of $\xi_{n,R}$ and $\xi_{n,L}$.) Similarly, as extensions of (3),

$$\sigma_R = \frac{\bar{n}_R + \frac{1}{2}}{Z_{\bar{n}_R,R}} \qquad \sigma_L = \frac{\bar{n}_L + \frac{1}{2}}{Z_{\bar{n}_L,L}}. \tag{6}$$

One could use (4)–(6) with specified left-hand and right-hand sidelobe levels and compute a pattern with asymmetric sidelobes, just as was done for the sum pattern in [3]. The result is, generally, a difference pattern in which the two main lobes are not quite at a common height, the boresight position is not quite at $z = 0$, and the differential between left-hand and right-hand sidelobe levels is systematically somewhat less than specified. Since all these minor defects can be overcome by the perturbation procedure used to obtain an arbitrary sidelobe topography, that is the course which will be pursued here, and (4) will be viewed as representing the starting pattern.

The perturbation procedure involves shifting the nulls to new positions

$$z_n = z_n{}^0 + \delta z_n \tag{7}$$

thus giving rise to the desired pattern

$$F(z) = C \cos \pi z \frac{\prod_{n=-(\bar{n}_L-1)}^{\bar{n}_R-1} (z_n - z)}{\prod_{n=0}^{\bar{n}_R-1} \left(1 - \frac{z}{n+\frac{1}{2}}\right) \prod_{n=0}^{\bar{n}_L-1} \left(1 + \frac{z}{n+\frac{1}{2}}\right)}. \tag{8}$$

In this procedure, $\bar{n}_R + \bar{n}_L - 1$ nulls are being repositioned. $\bar{n}_R - 1$ near-in sidelobes on the right side are affected; $\bar{n}_L - 1$ near-in sidelobes on the left side are affected; in addition, the two main lobes are perturbed. When one counts main lobes and sidelobes, the total is $\bar{n}_R + \bar{n}_L$. If the level of the right-hand main lobe is taken as reference, one sees that the relative levels of $\bar{n}_R + \bar{n}_L - 1$ lobes are being adjusted by shifting $\bar{n}_R + \bar{n}_L - 1$ null positions; thus the procedure is deterministic.

It is also necessary to provide a link between the level of the desired pattern $F(z)$ and the starting pattern $F_0(z)$. This can be done by requiring that the peak values of the right-hand main lobes in both patterns be the same. One can accomplish this by appropriate adjustment of δC in

$$C = C_0 + \delta C. \tag{9}$$

When (7) and (9) are inserted in (8), the first-order result is

$$F(z) = F_0(z) \left[1 + \frac{\delta C}{C_0} + \sum_{n=-(\bar{n}_L-1)}^{\bar{n}_R-1} \frac{\delta z_n}{z_n{}^0 - z}\right]. \tag{10}$$

Let the mth peak (main lobe or sidelobe) in the starting pattern occur at $z = y_m$. Then $F_0(y_m) = \eta_m{}^0$ is the field strength of this lobe. If the perturbations are small, $F(y_m) = \eta_m$ is approximately the field strength of the mth lobe in the desired pattern. Thus, from (10),

$$\frac{\eta_m}{\eta_m{}^0} - 1 = 1 + \frac{\delta C}{C_0} + \sum_{n=-(\bar{n}_L-1)}^{\bar{n}_R-1} \frac{\delta z_n}{z_n{}^0 - y_m} \tag{11}$$

in which m ranges from $-\bar{n}_L$ to $+\bar{n}_R$, excluding zero.

Equations (11) constitute a set of $\bar{n}_R + \bar{n}_L$ simultaneous linear equations in which all the $\eta_m, \eta_m{}^0, z_n{}^0, y_m$ values are known, and in which there are $\bar{n}_R + \bar{n}_L$ unknowns [δC plus the $(\bar{n}_R + \bar{n}_L - 1)$ perturbations δz_n]. Since C_0 can be taken as unity with no loss in generality, the set is complete.

With the establishment of (11), the remainder of the perturbation procedure is quite similar to what has been done earlier in the case of the sum pattern. Here, one can normalize both patterns by letting $\eta_1{}^0 = \eta_1 = 1$. The values of δC and δz_n are then computed and used in (8) to calculate the first iterative attempt at obtaining the desired pattern. If this initial result is not adequate, the first iteration is used as a new starting pattern and the whole procedure is repeated. A reasonable number of iterations will usually yield an acceptable approximation to the desired pattern. Several examples are offered in the next section.

EXAMPLES OF THE PERTURBATION PROCEDURE

Case 1

As an illustration of the use of the iterative technique developed in the previous section, let the desired pattern be a Bayliss 30/30 except that the second sidelobe on the right side is to be depressed to −40 dB.

Obviously, the appropriate starting pattern is the Bayliss 30/30, whose roots were given earlier in Table II. The pattern itself was shown in Fig. 1. The computer, working with (1), and using the roots listed in Table II, provides through a subroutine the amplitudes and positions of the lobe peaks in the Bayliss pattern. These are shown in Table III.

In this example, we wish to have $\eta_m = \eta_m{}^0$ except for $m = 2$. To get that lobe down to −40 dB, we choose $|\eta_2| = 0.01$. When this information is used in (11), the computer is able to determine the nineteen δz_n perturbations and δC. When these results are used in (7) and (9), and ultimately in (8), the first iteration $F(z)$ emerges. This is shown in Fig. 2(a) and is seen to be a good step toward the desired pattern.

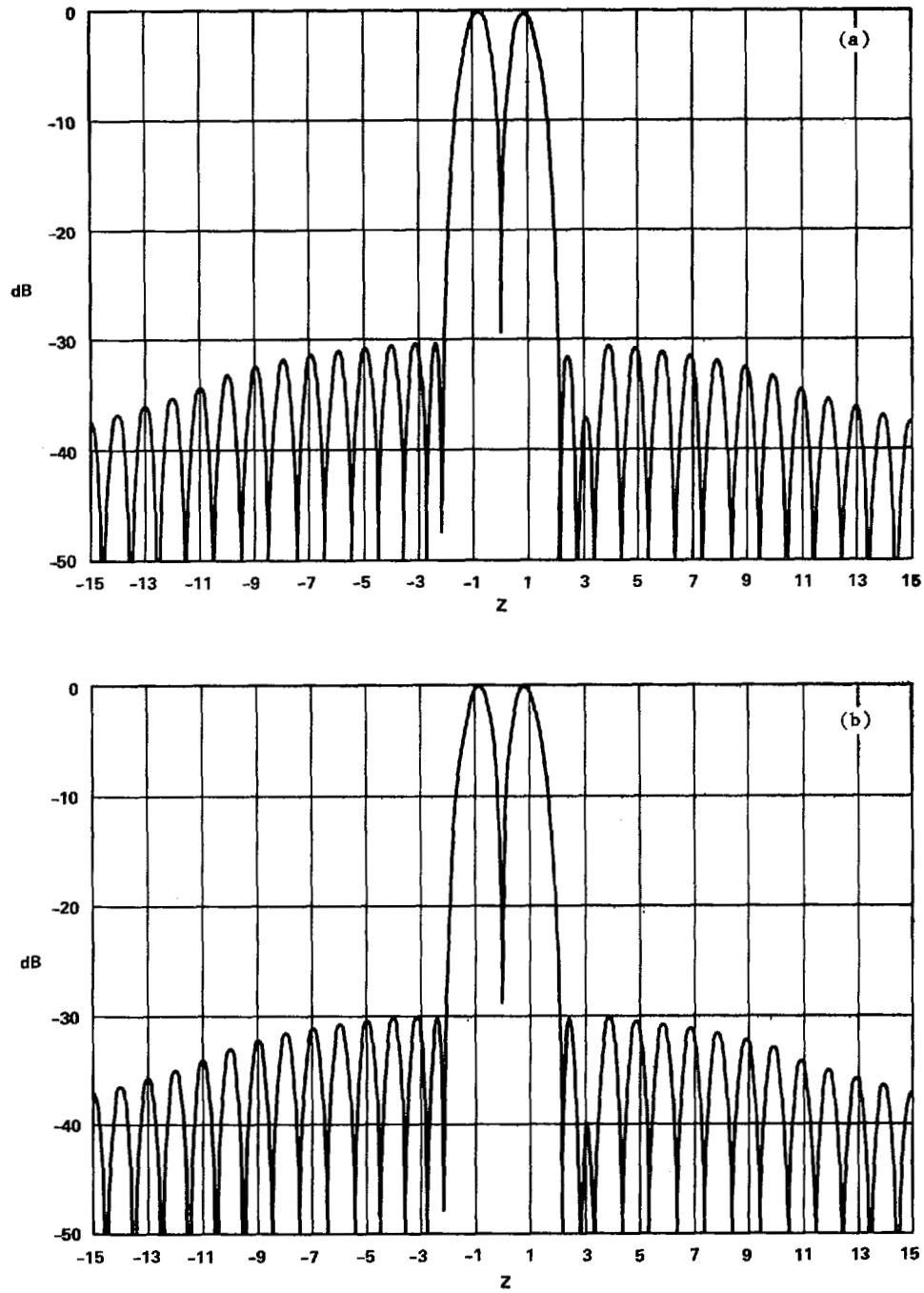

Fig. 2. Bayliss 30/30 pattern except for one lobe depressed to 40 dB.

With Fig. 2(a) used as the new starting pattern, two iterations of the process lead to Fig. 2(b) in which all lobes are within one quarter dB of specification.

Case 2

As a further illustration of the design procedure, let it be desired to create a pattern which is Bayliss 30/30 except that the first four sidelobes on both sides of the two main peaks are at -40 dB.

With the Bayliss 30/30 once again used as starting pattern, the sequence shown in Fig. 3 results. Only three iterations were needed to get all lobes within one quarter dB of specification.

The Aperture Distributions

If the aperture has the extent $-a \leq x \leq a$ and the normalized aperture variable is denoted by $p = \pi x/a$, then the pattern is given by

$$F(z) = \int_{-\pi}^{\pi} g(p) e^{ipz}\, dp \tag{12}$$

in which $g(p)$ is the aperture distribution function.

The Fourier series representation

$$g(p) = \frac{1}{2\pi} \sum_{m=-\infty}^{\infty} D_m e^{-i(m+1/2)p} \tag{13}$$

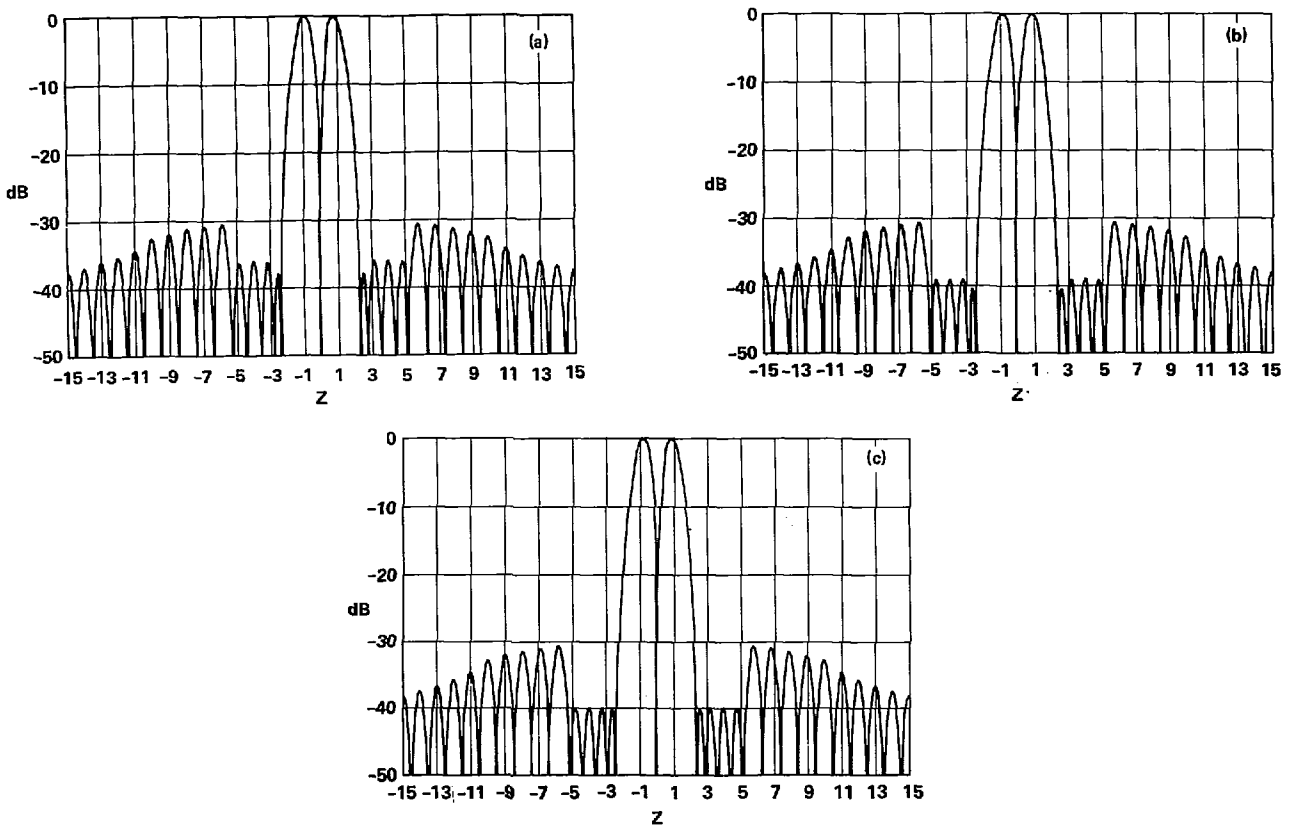

Fig. 3. Bayliss 30/30 pattern except four inner lobes on each side are depressed to 40 dB.

leads to

$$F(z) = \frac{1}{2\pi} \sum_{m=-\infty}^{\infty} D_m \int_{-\pi}^{\pi} e^{ip[z-(m+1/2)]}\, dp$$

$$= \sum_{m=-\infty}^{\infty} D_m \frac{\sin \pi[z - (m + \frac{1}{2})]}{\pi[z - (m + \frac{1}{2})]} \tag{14}$$

so that

$$F(n + \tfrac{1}{2}) = D_n. \tag{15}$$

Thus the aperture distribution function may be written as

$$g(p) = \frac{1}{2\pi} \sum_{-(\bar{n}_L - 1)}^{\bar{n}_R - 1} F(n + \tfrac{1}{2}) e^{-i(n+1/2)p}. \tag{16}$$

The series (16) truncates as shown because $F(n + \frac{1}{2}) = 0$ for n an integer beyond this range.

If one attempts to compute $F(n + \frac{1}{2})$ from (8) an indeterminacy of the form 0/0 arises. This can be resolved by standard means, the result being, for $0 \leq m \leq \bar{n}_R - 1$

$$F(m + \tfrac{1}{2}) = (-1)^m (m + \tfrac{1}{2})\pi C \cdot \frac{\prod_{-(\bar{n}_L-1)}^{\bar{n}_R-1} [z_n - (m + \frac{1}{2})]}{\prod_{\substack{n=0 \\ n \neq m}}^{\bar{n}_R-1} \left(1 + \frac{m + \frac{1}{2}}{n + \frac{1}{2}}\right) \prod_{n=0}^{\bar{n}_L-1} \left(1 + \frac{m + \frac{1}{2}}{n + \frac{1}{2}}\right)}. \tag{17}$$

In the range $-\bar{n}_L \leq m \leq -1$ the result is

$$F(m + \tfrac{1}{2}) = (-1)^m (m + \tfrac{1}{2})\pi C \cdot \frac{\prod_{-(\bar{n}_L-1)}^{\bar{n}_R-1} [z_n - (m + \frac{1}{2})]}{\prod_{n=0}^{\bar{n}_R-1} \left(1 - \frac{m + \frac{1}{2}}{n + \frac{1}{2}}\right) \prod_{\substack{n=0 \\ n \neq -(m+1)}}^{\bar{n}_L-1} \left(1 + \frac{m + \frac{1}{2}}{n + \frac{1}{2}}\right)}. \tag{18}$$

With the normalized aperture divided into 120 intervals ($\Delta p = \pi/60$), $g(p)$ was computed from (17) at each interval's end point for the Bayliss 30/30 pattern and for many cases which have been studied, including the two whose final patterns are shown in Figs. 2(b) and 3(c). The aperture distribution corresponding to Fig. 2(b) is tabulated in Table IV. Also listed is the distribution for the Bayliss 30/30. One can conclude from a study of Table IV that the two patterns are comparably difficult to achieve, but that to be able to shift from one to the other is beyond present state of the art.

Fig. 4 shows the aperture distribution corresponding to the pattern of Fig. 3(c), in which the four inner sidelobes on each side are depressed to -40 dB. Since this is a symmetric pattern, the phase is uniform except for the 180° jump at $p = 0$. The amplitude is symmetric, has a null at the center, and a small rise at the ends. This amplitude distribution is significantly different from the 30/30 Bayliss,

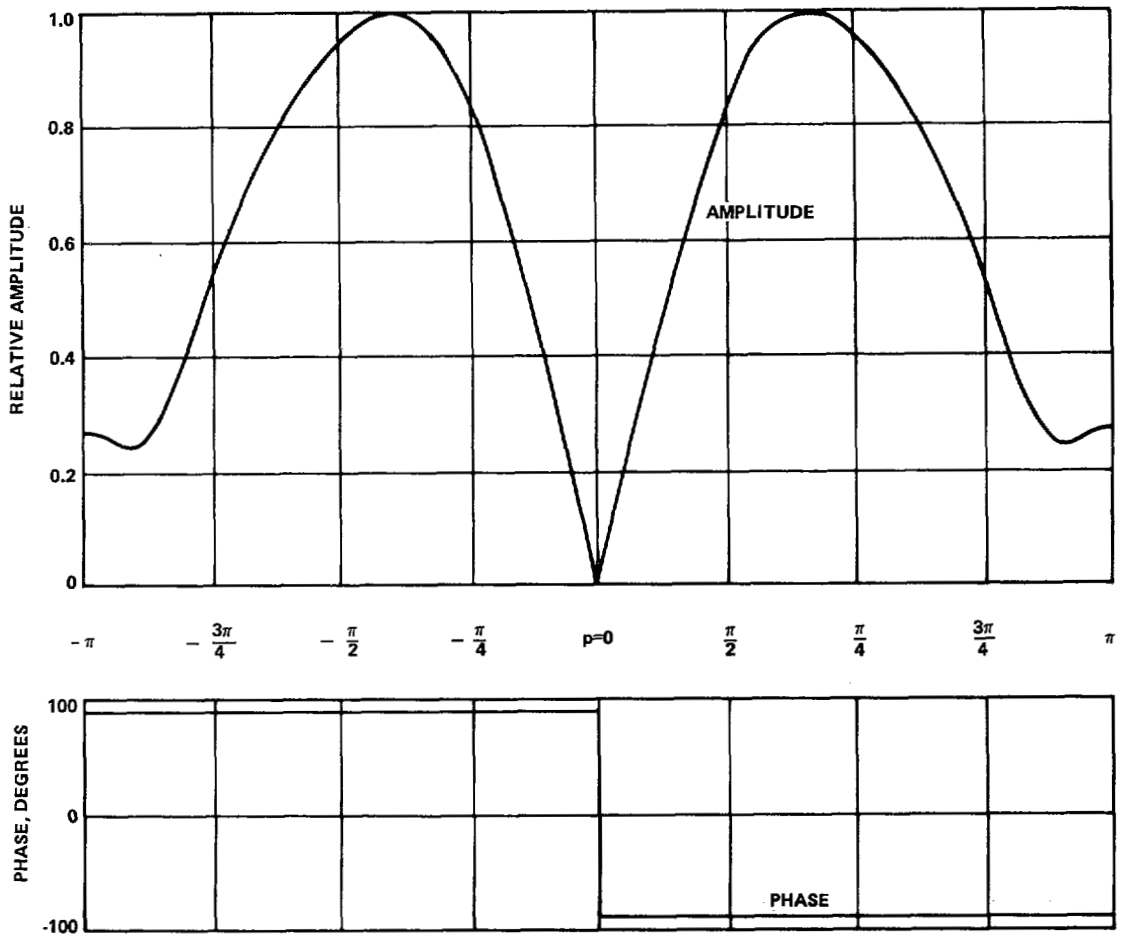

Fig. 4. Aperture distribution for perturbed Bayliss pattern of Fig. 3(c) with four inner lobes each side at -40 dB.

TABLE IV
APERTURE DISTRIBUTIONS FOR BAYLISS 30/30 AND FOR SUPPRESSION OF ONE SIDELOBE TO -40 dB

	Bayliss 30/30		One Lobe at -40 dB	
p†	$\lvert g(p)\rvert$	arg $g(p)$	$\lvert g(p)\rvert$	arg $g(p)$
$-\pi$	0.3456	90°	0.3343	90°
$-11/12\pi$	0.3616	90	0.3437	89.0
$-5/6\pi$	0.4591	90	0.4333	87.3
$-3/4\pi$	0.6292	90	0.6044	86.8
-2.3π	0.7855	90	0.7676	86.8
$-7/12\pi$	0.9093	90	0.9006	87.3
$-1/2\pi$	0.9871	90	0.9855	88.0
$-5/12\pi$	0.9938	90	0.9939	88.7
$-1/3\pi$	0.9265	90	0.9239	89.4
$-1/4\pi$	0.7804	90	0.7735	89.7
$-1/6\pi$	0.5636	90	0.5549	89.9
$-1/12\pi$	0.2963	90	0.2903	89.8
0	0	0	0	0

† Only half the aperture distribution is listed. $\lvert g(p)\rvert$ is symmetric and arg $g(p)$ antisymmetric in p for both distributions.

particularly in the end regions, and its physical realization is well within the state of the art.

DISCUSSION

Quite obviously, the rapidity of convergence from the starting pattern to the desired pattern depends on the complexity of the desired pattern. But it also depends on the choice of starting pattern. More rapid convergence would have resulted in Case 2 if a Bayliss 35/35 pattern had been chosen to initiate the process. However, the 30/30 Bayliss was already available and, as has been seen, only three iterations were needed anyway. More generally, if one desires to control $(\bar{n}_L - 1)$ sidelobes on the left side and $(\bar{n}_R - 1)$ sidelobes on the right side of the twin peaks in a difference pattern, it is best to use those values of $\bar{n}_L$ and $\bar{n}_R$ in (4) and to select A_L and A_R so that the left-hand and right-hand sidelobe levels in the starting pattern approximate the corresponding average sidelobe levels of the controlled sidelobes in the desired pattern.

It should be emphasized that the aperture distributions generated by this technique are for *continuous* line sources. Discrete linear arrays can result from sampling these continuous distributions. The complexity of the desired pattern is reflected in the complexity of the aperture distribution, which in turn dictates the maximum sampling interval.

Pattern multiplication permits the foregoing procedures to be extended to planar apertures.

CONCLUSIONS

A design technique has been described which will yield difference patterns with arbitrary sidelobe topographies, together with the requisite continuous aperture distributions.

The technique involves an inexpensive do-loop computer routine which has been found to provide rapid convergence from a starting pattern to a desired pattern for cases of practical interest. For some of these practical cases, the corresponding aperture distributions are well within current state of the art.

Acknowledgment

The author wishes to thank Mr. R. M. Johnson of Hughes for his invaluable help in computer programming.

References

[1] T. T. Taylor, "Design of line-source antennas for narrow beamwidth and low side lobes," *Trans. IRE*, vol. AP-3, pp. 16–28, January 1955.
[2] E. T. Bayliss, "Design of monopulse antenna difference patterns with low side lobes," *Bell Syst. Tech. J.*, vol. 47, pp. 623–650, May–June 1968.
[3] R. S. Elliott, "Design of line-source antennas for narrow beamwidth and low asymmetric side lobes," *Trans. IEEE*, vol. AP-23, pp. 100–107, January 1975.
[4] ——, "Design of line-source antennas for sum patterns with sidelobes of individually arbitrary heights," *Trans. IEEE*, vol. AP-24, January 1976.

Succinct Papers

Analysis of the Symmetric Center-Fed V-Dipole Antenna

J. EARL JONES, MEMBER, IEEE

***Abstract*—A wire antenna moment method using piecewise sinusoidal expansion and testing functions is used to obtain properties of a symmetric center-fed V-dipole antenna driven by a slice generator. The impedance, admittance, current distribution, radiation patterns in the dipole plane, and other properties are computed as functions of the parameters $0 < h/\lambda \leq 0.60$, $100 \leq h/a \leq 20\,000$, and $30° \leq \psi \leq 180°$, where h = arm length, λ = free space wavelength, a = wire radius, and ψ = apex angle. The results are checked with experiment and compared with similar results previously reported for the linear dipole. It is shown that 1) omnidirectional patterns over a wide bandwidth are achieved for $\psi \leq 90°$, but at the expense of reduced resonant radiation resistance and reduced bandwidth, insofar as the impedance is concerned, 2) for ψ less than about 75°–80°, lowest resonant length $\geq \lambda/4$ and increases as h/a decreases, and 3) lowest antiresonant length for $\psi > 30°$ is within 0.01λ of that for a linear dipole with the same h/a.**

I. Introduction

A symmetric center-fed V-dipole antenna is characterized geometrically by three basic parameters: arm length h, wire radius a, and apex angle ψ. Electromagnetic properties of the linear dipole, which is a special case of the V-dipole for $\psi = 180°$, have been studied extensively over the years, as excellent historical summaries attest [1, pp. 1–11], [2]. However, comparatively few studies of the V-dipole have been made [1, pp. 381–395, pp. 687–691], [2]–[8].

The determination of linear dipole properties, particularly the driving point impedance, has been facilitated analytically by treating the antenna as a boundary value problem and solving the appropriate integral equation (IE) for the current distribution. The earliest IE solutions for the linear dipole were obtained for the mathematically attractive, but historically controversial [1, pp. 1–8], [9] case for which the driving source is assumed to be a slice voltage generator across a gap of infinitesimal width (a delta-gap), and the King–Middleton second-order solution (KM2) [1, pp. 149–193] was used to obtain an extensive set of impedance computations from which various properties were derived.

A similar study for the symmetric center-fed V-dipole does not appear to be available, although King [1, pp. 381–387] did develop an IE formulation for the case for which each arm is represented by a thin right-circular cylinder of length h and radius a. The gap face of each cylinder is located a short distance δ from the point of intersection of the cylinder center lines and ψ is the angle between the center lines. For $\psi = 180°$ and $\delta = 0$, King's formulation reduces to that for a delta-gap linear antenna. For $\psi < 180°$, a delta-gap V-dipole cannot be treated because $\delta \neq 0$ unless $a \to 0$. Only when the cylinders are oblique, resulting in elliptical gap faces, is it possible for a delta-gap V-dipole to be represented.

Although King noted that his IE could be solved iteratively similar to KM2, no computations of the current distribution or radiation patterns were made. The only impedance computations made, which were a plot of impedance versus ψ for a half-wave V-dipole [1, p. 389], were based on a zero-order solution (KZ0), valid for $a \to 0$.

In this paper, an IE for the symmetric center-fed V-dipole delta-gap model (with elliptical faces for $\psi \neq 180°$) is solved implicitly by application of the piecewise sinusoidal reaction method (a Galerkin type moment method using piecewise sinusoidal expansion and testing functions) of Richmond [10]–[12]. However, in this paper the coefficients in the impedance matrix $[Z]$ of the equation $[Z][I] = [V]$ associated with this method are computed using Runge–Kutta numerical integration in lieu of the more efficient equations (using sine, cosine, and exponential integrals) which were unavailable when this study was conducted.

As functions of the parameters h/λ, h/a, and ψ, the following quantities are computed: a) driving point impedance $Z(h/\lambda, h/a,\psi) = R + jX$, where R and X are the resistance and reactance, respectively, b) driving point admittance $Y(h/\lambda,h/a,\psi) = 1/Z = G + jB$, where G and B are the conductance and susceptance, respectively, c) magnitude and phase of the current distribution, d) radiation patterns in the dipole plane, and e) other properties known as "critical parameters" [1, p. 152].

Manuscript received May 6, 1975; revised November 4, 1975. Portions of this work were presented at the 1972 International Antennas and Propagation Symposium, Williamsburg, VA, December 11–15.
The author was with NASA Langley Research Center, Hampton, VA. He is now with the U.S. Air Force Wright Aeronautical Laboratories Wright-Patterson Air Force Base, Dayton, OH 45433.